Effect of External Cooling on ^{177}Lu-PSMA Uptake by the Parotid Glands

Burcak Yilmaz[1], Serap Nisli[1], Nurhan Ergul[1], Riza Umar Gursu[2], Ozgur Acikgoz[3], and Tevfik Fikret Çermik[1]

[1]*Nuclear Medicine Department, Istanbul Research and Training Hospital, University of Health Sciences, Istanbul, Turkey;* [2]*Medical Oncology Department, Istanbul Research and Training Hospital, University of Health Sciences, Istanbul, Turkey; and* [3]*Medical Oncology Department, Kanuni Sultan Suleyman Research and Training Hospital, University of Health Sciences, Istanbul, Turkey*

Recent years have seen the start of treatment of metastatic castration-resistant prostate cancer with prostate-specific membrane antigen (PSMA)–targeted radioligand therapy (PRLT), especially ^{177}Lu-PSMA-617. However, PRLT has side effects on the salivary glands that limit the safety of the treatment. The current study aimed to show the effect of external cooling with ice packs on ^{177}Lu-PSMA-617 uptake by the parotid glands (PGs). **Methods:** The study included 19 patients (mean age, 72.9 y) with metastatic castration-resistant prostate cancer who had been referred for the first time for ^{177}Lu-PSMA-617 treatment and underwent pretreatment ^{68}Ga-PSMA-11 PET/CT. Before the initiation of PRLT, the SUV_{max} and SUV_{mean} of the right and left PGs were measured on ^{68}Ga-PSMA PET/CT. Frozen ice packs were then affixed over the right PG of each patient for approximately 5 h; 1 h after they were affixed, PRLT was administered. At 4 h after PRLT, head-and-neck SPECT/CT was performed, and at both 4 and 24 h after PRLT, whole-body planar scintigraphy was performed. Regions and volumes of interest were applied for the right and left PGs, and the counts and volumes were determined. **Results:** Before PRLT, ^{68}Ga-PSMA-11 PET/CT showed no significant difference in SUV_{max} or SUV_{mean} between the right and left PGs ($P > 0.05$). At 4 and 24 h after PRLT, planar imaging showed no significant difference in counts between the cooled and noncooled PGs ($P > 0.05$). Furthermore, at 4 h after PRLT, SPECT/CT showed no significant difference in counts or volumes between the cooled and noncooled PGs ($P > 0.05$). **Conclusion:** External cooling does not reduce uptake of ^{177}Lu-PSMA-617 by the PGs.

Key Words: ^{177}Lu; PSMA; prostate cancer; parotid; ice-pack

J Nucl Med 2019; 60:1388–1393
DOI: 10.2967/jnumed.119.226449

Although many treatment modalities have been developed for metastatic castration-resistant prostate cancer (mCRPC), expected survival for patients is usually less than 20 mo (*1*). Prostate-specific membrane antigen (PSMA), which is a 750-amino-acid type II transmembrane glycoprotein, is a promising target for diagnosis of mCRPC with ^{68}Ga and radioligand therapy with ^{177}Lu (*2–7*). Besides, prostate carcinoma cells, especially poorly differentiated types, express PSMA at levels up to 100–1,000 times higher than benign prostate tissue (*7–9*), making them an ideal and important target for imaging and treatment modalities (*3,9–11*).

^{68}Ga-PSMA-11 PET/CT is a highly sensitive and specific diagnostic tool, especially in poorly differentiated prostate carcinoma, and also provides valuable information that can be used to select patients for PSMA-targeted radioligand therapy (PRLT) and therapy monitoring (*12*). Treatment of mCRPC with PRLT has begun in recent years (*12,13*). PRLT with ^{177}Lu-PSMA is safe and has relatively low toxicity (*5,14–19*). ^{177}Lu-PSMA-617 is a low-molecular-weight ligand that binds to the cell surface of prostate carcinoma cells and is transported into the cell by receptor-mediated endocytosis, emitting short-range β-particles (*20*) that provide local irradiation of both primary tumor and metastases, as well as tumor radiation and γ-emission that allow uptake quantification by scintigraphy thereafter (*7,21*). However, the PSMA receptor is expressed at high levels in normal tissues such as the kidneys (proximal tubules), the jejunum (brush border), and the salivary and lacrimal glands (*2,21–23*).

The salivary glands are radiosensitive organs, and physiologic high binding of PSMA ligands may cause undesirable side effects (*19,24*). Xerostomia, a frequent but mild to moderate side effect after PRLT of mCRPC, decreases the patient's quality of life (*19,25–27*). One suggestion has been the use of external cooling to bring about vasoconstriction, reduce blood flow, decrease PSMA binding, and thus prevent radiation toxicity to the salivary glands (*5,14,16,18,28–32*). Transient xerostomia or hypogeusia was reported in 4%–87% of patients with or without external cooling with ice packs (*14,26,31,33*). In a recently published study, ^{68}Ga-PSMA-11 PET/CT salivary gland uptake was suggested to be a simulation model just before PRLT (*7*). To date, there has been no established evidence that cooling indeed decreases ^{177}Lu-PSMA-617 uptake by the salivary glands. In the present study, we aimed to clarify the effect of cooling with ice packs on ^{177}Lu-PSMA-617 uptake by the parotid glands (PGs).

MATERIALS AND METHODS

Study Population

mCRPC patients who had been referred for ^{177}Lu-PSMA-617 PRLT and had undergone pretreatment ^{68}Ga-PSMA-11 PET/CT were included in this prospective investigational study from May 2018 to October 2018. Patients were excluded if they had a previous or concurrent diagnosis of any other primary malignancy, had been pretreated with radiotherapy to the head and neck, had been previously treated with PRLT, had renal or urinary disorders, or could not apply

Received Jan. 23, 2019; revision accepted Mar. 4, 2019.
For correspondence or reprints contact: Burcak Yilmaz, University of Health Sciences, Kasap İlyas Mah., Org. Abdurrahman Nafiz Gürman Cd., Fatih, Istanbul 34098, Turkey.
E-mail:drburcak@gmail.com
Published online Mar. 8, 2019.

the ice pack. Additionally, patients were excluded if more than 45 d had elapsed between PRLT and pretreatment ^{68}Ga-PSMA-11 PET/CT. Nineteen patients (mean age, 72.9 y; range, 62–81 y) who underwent routine clinical staging, including physical and urologic examination, complete blood count, and biochemical tests, were included in the current study. The local ethics committee approved this study (2018-1419), and all subjects gave written informed consent.

^{68}Ga-PSMA-11 PET/CT Examination and Analysis

The ^{68}Ga-PSMA-11 was synthesized in-house using a Trasis synthesis module with an ITG semiautomated generator. The compound was stable in vitro and had a radiochemical purity of more than 99% after 2 h of radiolabeling. In-house–generated ^{68}Ga-PSMA-11 (median, 175 MBq; range, 77–350 MBq) was injected intravenously, and the patients rested in a comfortable, quiet room during the uptake phase. They were asked to empty their bladder immediately before the scan. No ice packs were applied before the PET/CT scan, which served as a control.

PET/CT images were acquired using an mCT 20 Excel lutetium oxyorthosilicate device (Siemens Molecular Imaging). Approximately 60 min after the ^{68}Ga-PSMA-11 injection, PET/CT was performed from the vertex to the mid thigh. The CT parameters were 140 kV, 80 mA, and a 3.75-mm slice thickness. PET was performed with the patients in the same position. The emission scan time was 3 min/bed position, and 6–7 bed positions covered the scanning range. Transaxial, sagittal, coronal, and fused images were analyzed on a workstation (Syngo.via; Siemens Molecular Imaging). Quantitative image analyses were performed by 2 nuclear medicine physicians with significant experience in reading ^{68}Ga-PSMA-11 PET/CT scans (average, 8 reads/mo individually). The SUV_{max} and SUV_{mean} of a 3-dimensional volume of interest were measured for the right and left PGs (Fig. 1). The salivary glands were delineated using a 10% threshold of the maximum pixel value within the volume of interest (isocontour) (*7,21*). Also, the SUV_{max} and SUV_{mean} of the cranium (around a region between the vertex and the glabella, for background values) were determined in areas where homogeneous uptake without any evidence of metastasis was observed. Measurements were corrected for lean body mass, according to the formula defined in the European Association of Nuclear Medicine guidelines (*34*).

Application of Ice Packs

One hour before the initiation of PRLT, 500 mL of intravenous hydration with saline was started. At the same time, frozen ice packs, covered with a dry towel, were affixed over the right PG of each patient. The ice packs were applied without cessation until 4 h after the treatment had ended (~5 h). The ice packs were replaced with fresh ones every 30 min.

Preparation and Administration of ^{177}Lu-PSMA-617

The ^{177}Lu-PSMA-617 was synthesized in-house using the Trasis synthesis module. The compound was stable in vitro and had a radiochemical purity of more than 99% after 2 h of radiolabeling. ^{177}Lu-PSMA-617 (mean, 5.3 ± 14.6 GBq; range, 3.7–7.7 GBq), diluted in 100 mL of physiologic saline was administered slowly in an intravenous infusion for over 15–20 min. After termination of the infusion, all patients received intravenous hydration (1,000 mL of 0.9% NaCl; flow, 250 mL/h) for 4 h.

Scintigraphy and Analysis

Whole-body and SPECT/CT imaging were performed using an AnyScan SPECT/CT scanner (Mediso Medical Imaging Systems) with a medium-energy general-purpose collimator, a 20% energy window, a peak at 208 keV, a scan speed of 15 cm/min for whole-body imaging, 32 frames with a 40-s exposure time per frame for each tomographic scan with 16-slice CT, and less than or equal to 10-kW nondiagnostic CT. Whole-body scintigraphy was performed at 4 and 24 h after PRLT, and head-and-neck SPECT/CT was performed at 4 h after PRLT.

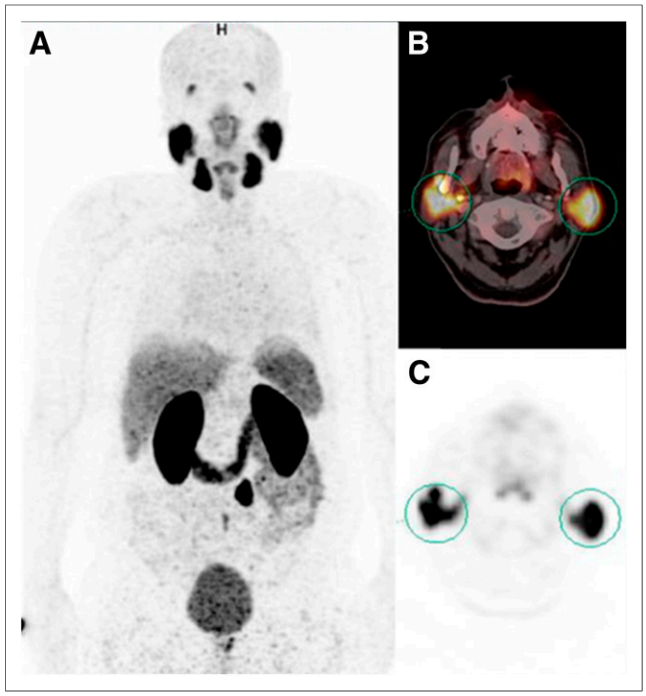

FIGURE 1. SUV_{max} and SUV_{mean} on ^{68}Ga-PSMA-11 PET/CT images of right and left PGs without any external cooling revealed no differences. Shown are maximum-intensity-projection PET (A), transaxial fused PET/CT (B), and CT (C) images, with region of interest or volume of interest on images.

Quantitative image analyses were performed by a nuclear medicine physician on a workstation (InterView Fusion Ultimate Processing Workstation with InterView XP Planar and InterView Fusion multimodality processing software). Regions of interest were drawn manually for the right and left PGs and the cranium (around the vertex–glabella, for background counts) for the 4- and 24-h anterior and posterior planar scintigraphic images (Fig. 2). Geometric means were calculated for each variable using the anterior and posterior counts. Also calculated were the volume of interest of the SPECT counts and the CT volume for the right and left PGs at 4 h (Fig. 3).

Statistical Analysis

All statistical analyses were performed using SPSS software (version 20.0; SPSS Inc.), with a P value of less than 0.05 considered to be significant. Paired t testing was used to compare right and left PG uptake for ^{68}Ga-PSMA-11 PET/CT variables (SUV_{max} and SUV_{mean}) without ice pack application and to compare 4- and 24-h right and left PG uptake on planar scintigraphy images after ice pack application. Also, 4-h SPECT volume-of-interest counts and volumes were compared between the right and left PGs using paired t testing. Furthermore, the right and left PG counts for the 4-h planar scintigraphic images and the right and left PG SUV_{max} and SUV_{mean} were divided by the background counts and the values for each patient to obtain right PG–to–cranium and left PG–to–cranium ratios. Paired t testing was used to compare the right ratios with the left ratios for planar counts, SUV_{max}, and SUV_{mean}.

RESULTS

Descriptive statistics for both the PET/CT and the SPECT/CT variables are shown in Table 1. A comparison of the right and left

FIGURE 2. Region-of-interest measurements on ^{177}Lu-PSMA-617 uptake (anterior [A]; posterior [B]) in both PGs and cranium in patient who was scanned with right-sided ice pack. No differences in radioligand uptake were observed when comparing cooled (right) and noncooled (left) sides, with region of interest or volume of interest on images.

PG count and volume variables according to application of ice packs and according to background is shown in Table 2.

Before PRLT, ^{68}Ga-PSMA-11 PET/CT without ice pack application showed no significant difference in SUV_{max} or SUV_{mean} between the right and left PGs ($P > 0.05$).

At 4 and 24 h after PRLT, the regions of interest for the cooled and noncooled PGs did not significantly differ ($P > 0.05$). Furthermore, at 4 h there was no significant difference in volume-of-interest counts on SPECT/CT between the right and left PGs. To dismiss intrapatient volume differences between the right and left PGs, we calculated the volumes of the right and left PGs and found no significant differences between them ($P > 0.05$).

Additionally, right PG–to–cranium and left PG–to–cranium count ratios were compared on 4-h scintigraphic images and no significant difference was found, nor could we find any significant difference between right PG–to–cranium and left PG–to–cranium SUV_{max} or between right PG–to–cranium and left PG–to–cranium SUV_{mean}.

DISCUSSION

The present study found no significant difference in ^{177}Lu-PSMA-617 uptake between cooled and noncooled PGs in the same patient. We thus conclude that external cooling of the salivary glands has no impact on PG PRLT uptake.

Although the proliferation rate of salivary gland cells is slow, they are radiosensitive (*19,35*). PRLT is a recently developed entity, but protection of the salivary glands from radiation has been of interest in the nuclear medicine literature since the time that the effects of radioiodine therapy on thyroid cancer patients were published (*36*). Because the mechanism by which radioiodine accumulates in the salivary glands is different from that of PSMA-targeted therapy, they require different methods of preventing radiation toxicity. ^{131}I emits 2 types of radiation, with β^- being used for treatment with a maximum energy of 812 keV (0.7%; 606 keV, 89.3%). Its physical half-life is 8.07 d, and the electrons penetrate soft tissue to a depth of about 1 mm, with a maximum of 2.4 mm (*37–39*). ^{177}Lu is a medium-energy β-emitter (490 keV) with a maximum energy of 0.5 MeV, a mean range of 0.7 mm and maximum range of 2.1 mm in soft tissue, and a half-life of 6.7 d (*40*). Although these properties are relatively similar for both radioactive isotopes, ^{177}Lu-PSMA uptake in the salivary glands is very high, with a transmembrane receptor-binding mechanism. For protection from radioiodine toxicity, sialogogues (e.g., vitamin E or lemon juice), pilocarpine, amifostine, or PG massage have been shown to significantly reduce damage to the salivary glands, whereas chewing gum has shown no protective effects (*36,41–47*). The main purpose of those trials was to prevent acute and chronic sialadenitis, xerostomia, and hypogeusia.

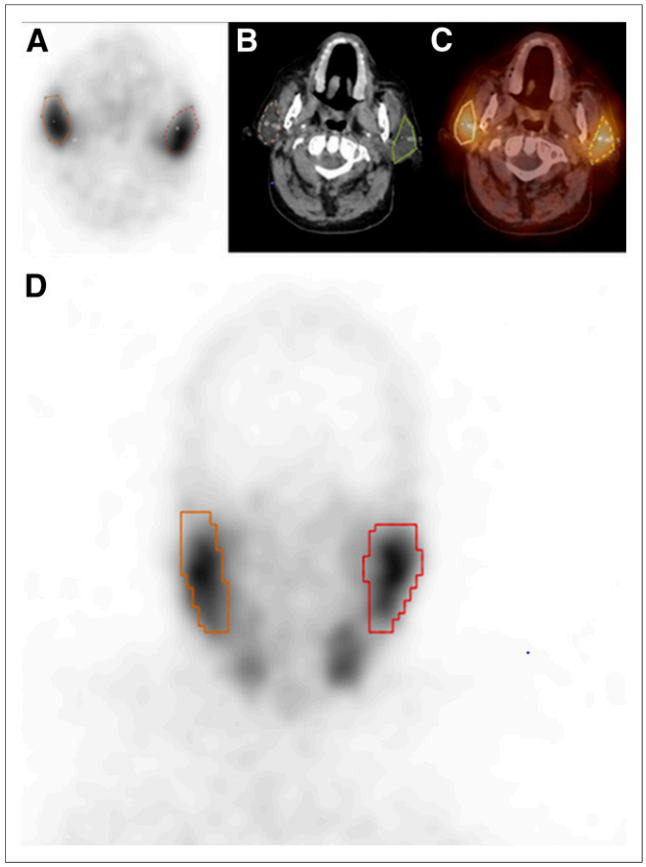

FIGURE 3. Volume-of-interest (count) and volume (mm^3) calculations of ^{177}Lu-PSMA-617 SPECT/CT images revealed no difference in either count or volume parameters. Shown are transaxial SPECT (A), CT (B), fused SPECT/CT (C), and coronal SPECT (D) images, with region of interest or volume of interest on images.

TABLE 1
Descriptive Variables of Patients

Variable	Mean ± SD	Range
Age (y)	72.9 ± 5.2	62–81
SPECT/CT variables		
R PG planar 4-h count	11,602 ± 5,811	1,749–28,073
L PG planar 4-h count	10,991 ± 6,016	2,116–20,545
R PG planar 24-h count	9,240 ± 5,540	1,350–24,389
L PG planar 24-h count	8,759 ± 5,374	883–20,056
R PG SPECT 4-h count	82,627 ± 49,428	29,199–187,765
L PG SPECT 4-h count	86,349 ± 53,180	36,320–190,580
R PG CT 4-h volume (mm^3)	17,820 ± 7,074	10,263–29,641
L PG CT 4-h volume (mm^3)	17,163 ± 6,715	8,696–29,259
Cranium planar AP (4-h) (count)	8,233 ± 4,782	2,298–19,972
^{68}Ga-PSMA PET/CT variables		
R PG SUV_{max}	17.1 ± 7.8	5.4–29.4
L PG SUV_{max}	17.6 ± 8.4	5.6–27.4
R PG SUV_{mean}	6.1 ± 4.4	2–18.9
L PG SUV_{mean}	5.8 ± 3.7	1.9–15.8
Liver SUV_{mean}	4.7 ± 1.6	1.7–7.6
Spleen SUV_{mean}	6.6 ± 1.6	3.9–9.3
Cranium SUV_{max}	2.1 ± 0.6	0.9–3.1
Cranium SUV_{mean}	0.2 ± 0.07	0.1–0.3

The salivary glands have the highest PSMA binding in normal, healthy tissues (*19,35*). Irreversible salivary gland damage from radiation toxicity is a concern of nuclear medicine physicians when planning PSMA-targeted therapies for mCRPC patients. Damage to the salivary glands and the development of xerostomia are a frequent side effect of radiation therapy and decrease the patient's quality of life (*19,35*). Although initial studies demonstrated that the salivary glands are not the dose-limiting organs, with a mean absorbed dose of 1.4 Gy/GBq of ^{177}Lu-PSMA-617, taking precautions to prevent salivary gland toxicity during targeted therapy has been recommended (*24,35*). In some recent studies, an ice-pack collar was used during ^{177}Lu-PSMA-617 treatment to induce vasoconstriction and reduce PSMA binding to the salivary glands (*5,14,16,30–32*). Transient xerostomia or hypogeusia was reported both in patients with and in patients without ice packs (*14,26,31*). In a recently published prospective study that did not use ice packs, grade 1 xerostomia was observed at a higher rate but there was no grade 3–4 toxicity in which symptoms needed to be relieved with salivary substitute gels (*33*). However, these studies evaluated only clinical results, without image-based analysis, and thus could not compare patient-based differences between PGs according to ice-pack application. On the other hand, these studies support the current study's finding of no difference in uptake between cooled and noncooled PGs.

van Kalmthout et al. investigated the effect of external cooling of the PGs on PSMA uptake on ^{68}Ga-PSMA-11 PET/CT and suggested that some significant differences in SUV_{max} and SUV_{peak} may exist between the cooled and noncooled PGs (*7*). Bohn et al. (*48*) also studied the effect that external cooling of the PGs has on PSMA uptake in patients undergoing ^{68}Ga-PSMA-11 PET/CT. These 2 studies claimed that external cooling with ice packs seems to reduce ^{68}Ga-PSMA-11 uptake in the PGs. The studies were only models, created to give an idea for PSMA-targeted therapies. Besides, PMSA ligands used for ^{68}Ga and ^{177}Lu differ, and the differences may cause different reactions across ice packs. However, in both ^{177}Lu-PSMA-617 treatment and ^{68}Ga-PSMA-11 imaging, the salivary glands have high uptake that may rule out any PSMA ligand differences. Ahmadzadehfar et al. (*15*) compared salivary gland function at baseline and after a single cycle of ^{177}Lu-PSMA-617 therapy, using dynamic salivary gland scintigraphy with ^{99m}Tc-pertechnetate, in order to see the protective effect of external cooling. Comparison of baseline with follow-up salivary gland scintigraphy did not show any change in salivary gland

TABLE 2
Statistical Analysis According to Ice-Pack Application

Variable	*P*	95% CI	SD
R/L PG planar (4-h)	0.572	−1,619–2,841	4,626.75
R/L PG planar (24-h)	0.314	−495–1,456	2,023.65
R/L PG SPECT (4-h)	0.270	−10,582–3,144	14,239.43
R/L PG CT volume (4-h)	0.481	−1,261–2,573	3,977.60
R/L PG SUV_{mean}	0.524	−0.67–1.27	2.00
R/L PG SUV_{max}	0.575	− 2.13−1.22	3.47
R-C/L-C PG planar (4-h)	0.104	−0.074–0.722	0.8
R-C/L-C PG SUV_{mean}	0.556	−2.5–4.56	7.4
R-C/L-C PG SUV_{max}	0.08	−2.39–0.13	2.6

CI = confidence interval; C = cranium.

uptake or clearance of ^{99m}Tc-pertechnetate, also supporting the findings of our study.

We know that the kinetics of the radiotracers differ. Therefore, modeling of ^{68}Ga-PSMA-11 for ^{177}Lu-PSMA may not give the same results. ^{68}Ga-PSMA-11 has a relatively rapid blood clearance and a relatively slow early elimination phase (*7,49*). On the other hand, ^{177}Lu-PSMA-617 has a long half-life, and uptake of ^{177}Lu-PSMA-617 from the interstitial or intracellular space into the salivary glands is relatively slow (*7*). Apart from these considerations, labeling of PSMA-targeting antibodies such as J591 instead of small molecules such as PSMA-617 (molecular weight, 150 vs. 1.4 kD, respectively) might be able to lower the PSMA uptake and decrease the risk of sialotoxicity (*25,50,51*).

It has been anticipated that reducing PSMA uptake by the salivary glands through a relatively short period of cooling may be even less effective in PSMA-targeted therapies and that long-term application of ice packs during the therapeutic procedure can be considered (*7*). In the present study, patients were exposed to external cooling for approximately 5 h—a relatively long period. Even this period of application was uncomfortable for the patients, who wanted to terminate the cooling procedure. Therefore, extending this cooling time would seem problematic.

New strategies have been suggested or developed to prevent salivary gland toxicity from PRLT. In a recent case report, intraparenchymal injections of 80 units of botulinum toxin into the PG unilaterally 45 d before ^{68}Ga-PSMA PET/CT was shown to decrease SUV_{mean} by up to 64%, compared with baseline (*52*). This approach needs further investigation, as it shows promise as a method of protecting the salivary glands from radiation during PSMA radioligand therapy. Short-acting anticholinergic agents and local anesthetics, injected into the salivary glands in preclinical trials, also gave promising data (*53*). Local application of cold compounds or inhibitors of PSMA, such as 2-(phosphonomethyl) pentanedioic acid, has been also investigated (*54*). Because of the high blood supply of the PGs, systemic absorption from intraparenchymal application of 2-(phosphonomethyl)pentanedioic acid may cause potential inhibition of PSMA-targeted tumor cells, which needs further consideration (*25*). Gene and stem cell therapy has been suggested to prevent xerostomia and may soon solve the problem (*24*). Besides, patient-specific dosimetry may help bring about successful tumor dosing and prevent organ toxicity (*19,35*).

To our knowledge, this was the first prospective study to compare the effect of external cooling on an intrapatient basis. To control the effect of external cooling, pretreatment differences in intrapatient analysis were possible with ^{68}Ga-PSMA PET/CT. Intrapatient volume-based analysis was calculated with SPECT/CT to eliminate volume-based differences. We also could compare the intrapatient effect of external cooling with exclusion of physiologic differences, which can differ from one patient to another.

CONCLUSION

External cooling of the PGs to reduce ^{177}Lu-PSMA-617 uptake with ice packs seems not to work. Alternative methods are needed to prevent PRLT effects on the salivary glands in patients undergoing ^{177}Lu-PSMA therapy.

DISCLOSURE

No potential conflict of interest relevant to this article was reported.

KEY POINTS

QUESTION: Does external cooling with ice packs really reduce uptake of ^{177}Lu-PSMA-617 in the PGs?

PERTINENT FINDINGS: In this prospective investigational study, external unilateral cooling of the PG in 19 prostate cancer patients treated with ^{177}Lu-PSMA-617 had no statistically significant effect when compared with the opposite gland, which was not cooled.

IMPLICATIONS FOR PATIENT CARE: External cooling of the PGs with ice packs does not reduce ^{177}Lu-PSMA-617 uptake. Alternative methods are needed to prevent PRLT effects on the salivary glands.

REFERENCES

1. Heidenreich A, Bastian PJ, Bellmunt J, et al. European Association of Urology. EAU guidelines on prostate cancer. Part 1: screening, diagnosis, and local treatment with curative intent—update 2013. *Eur Urol.* 2014;65:124–137.
2. Afshar-Oromieh A, Hetzheim H, Kratochwil C, et al. The theranostic PSMA ligand PSMA-617 in the diagnosis of prostate cancer by PET/CT: biodistribution in humans, radiation dosimetry, and first evaluation of tumor lesions. *J Nucl Med.* 2015;56:1697–1705.
3. Afshar-Oromieh A, Malcher A, Eder M, et al. PET imaging with a [Ga-68] gallium-labelled PSMA ligand for the diagnosis of prostate cancer: biodistribution in humans and first evaluation of tumour lesions. *Eur J Nucl Med Mol Imaging.* 2013;40:486–495.
4. Ahmadzadehfar H, Azgomi K, Hauser S, et al. ^{68}Ga-PSMA-11 PET as a gatekeeper for the treatment of metastatic prostate cancer with ^{223}Ra: proof of concept. *J Nucl Med.* 2017;58:438–444.
5. Ahmadzadehfar H, Wegen S, Yordanova A, et al. Overall survival and response pattern of castration-resistant metastatic prostate cancer to multiple cycles of radioligand therapy using [^{177}Lu]Lu-PSMA-617. *Eur J Nucl Med Mol Imaging.* 2017;44:1448–1454.
6. Rajasekaran AK, Anilkumar G, Christiansen JJ. Is prostate specific membrane antigen a multifunctional protein? *Am J Physiol Cell Physiol.* 2005;288:C975–C981.
7. van Kalmthout LWM, Lam MGEH, de Keizer B, et al. Impact of external cooling with icepacks on ^{68}Ga-PSMA uptake in salivary glands. *EJNMMI Res.* 2018;8:56.
8. Silver DA, Pellicer I, Fair WR, Heston WD, Cordon-Cardo C. Prostate-specific membrane antigen expression in normal and malignant human tissues. *Clin Cancer Res.* 1997;3:81–85.
9. Wright GL Jr, Haley C, Beckett ML, Schellhammer PF. Expression of prostate specific membrane antigen in normal, benign, and malignant prostate tissues. *Urol Oncol.* 1995;1:18–28.
10. Ghosh A, Heston WD. Tumor target prostate specific membrane antigen (PSMA) and its regulation in prostate cancer. *J Cell Biochem.* 2004;91:528–539.
11. Zang J, Fan X, Wang H, et al. First-in-human study of ^{177}Lu-EB-PSMA-617 in patients with metastatic castration-resistant prostate cancer. *Eur J Nucl Med Mol Imaging.* 2019;46:148–158.
12. Kulkarni HR, Singh A, Schuchardt C, et al. PSMA-based radioligand therapy for metastatic castration-resistant prostate cancer: the Bad Berka experience since 2013. *J Nucl Med.* 2016;57(suppl 3):97S–104S.
13. Baum RP, Kulkarni HR, Schuchardt C, et al. ^{177}Lu-labeled prostate-specific membrane antigen radioligand therapy of metastatic castration-resistant prostate cancer: safety and efficacy. *J Nucl Med.* 2016;57:1006–1013.
14. Ahmadzadehfar H, Eppard E, Kurpig S, et al. Therapeutic response and side effects of repeated radioligand therapy with ^{177}Lu-PSMA-DKFZ-617 of castrate-resistant metastatic prostate cancer. *Oncotarget.* 2016;7:12477–12488.
15. Ahmadzadehfar H, Rahbar K, Kurpig S, et al. Early side effects and first results of radioligand therapy with ^{177}Lu-DKFZ-617 PSMA of castrate-resistant metastatic prostate cancer: a two-centre study. *EJNMMI Res.* 2015;5:114.
16. Rahbar K, Schmidt M, Heinzel A, et al. Response and tolerability of a single dose of ^{177}Lu-PSMA-617 in patients with metastatic castration-resistant prostate cancer: a multicenter retrospective analysis. *J Nucl Med.* 2016;57:1334–1338.
17. Kratochwil C, Giesel FL, Stefanova M, et al. PSMA-targeted radionuclide therapy of metastatic castration-resistant prostate cancer with ^{177}Lu-labeled PSMA-617. *J Nucl Med.* 2016;57:1170–1176.
18. Fendler WP, Rahbar K, Herrmann K, Kratochwil C, Eiber M. ^{177}Lu-PSMA radioligand therapy for prostate cancer. *J Nucl Med.* 2017;58:1196–1200.

19. Awang ZH, Essler M, Ahmadzadehfar H. Radioligand therapy of metastatic castration-resistant prostate cancer: current approaches. *Radiat Oncol.* 2018;13:98.
20. Bé MM, Chisté V, Dulie C, et al. Table of radionuclides (vol. 2-A = 151 to 242). Bureau International des Poids et Mesures website. https://www.bipm.org/utils/common/pdf/monographieRI/Monographie_BIPM-5_Tables_Vol2.pdf. Published 2004. Accessed June 4, 2019.
21. Hohberg M, Eschner W, Schmidt M, et al. Lacrimal glands may represent organs at risk for radionuclide therapy of prostate cancer with [^{177}Lu]DKFZ-PSMA-617. *Mol Imaging Biol.* 2016;18:437–445.
22. Ristau BT, O'Keefe DS, Bacich DJ. The prostate-specific membrane antigen: lessons and current clinical implications from 20 years of research. *Urol Oncol.* 2014;32:272–279.
23. Klein Nulent TJW, Valstar MH, de Keizer B, et al. Physiologic distribution of PSMA-ligand in salivary glands and seromucous glands of the head and neck on PET/CT. *Oral Surg Oral Med Oral Pathol Oral Radiol.* 2018;125:478–486.
24. Taïeb D, Foletti JM, Bardiès M, Rocchi P, Hicks RJ, Haberkorn U. PSMA-targeted radionuclide therapy and salivary gland toxicity: why does it matter? *J Nucl Med.* 2018;59:747–748.
25. Langbein T, Chaussé G, Baum RP. Salivary gland toxicity of PSMA radioligand therapy: relevance and preventive strategies. *J Nucl Med.* 2018;59:1172–1173.
26. Rahbar K, Ahmadzadehfar H, Kratochwil C, et al. German multicenter study investigating ^{177}Lu-PSMA-617 radioligand therapy in advanced prostate cancer patients. *J Nucl Med.* 2017;58:85–90.
27. Langbein T, Kulkarni HR, Singh A, Baum RP. Functional imaging of the salivary glands for evaluation of radiation-induced sialadenitis before and after Lu-177 PSMA radioligand therapy [abstract]. *Eur J Nucl Med Mol Imaging.* 2017; 44(suppl 2):328.
28. Braat A, Ahmadzadehfar H. Lutetium-177 labelled PSMA ligands for the treatment of metastatic castrate-resistant prostate cancer. *Tijdschr Nucl Geneeskd.* 2017;38:1627–1634.
29. Boellaard R, Delgado-Bolton R, Oyen WJG, et al. FDG PET/CT: EANM procedure guidelines for tumour imaging: version 2.0. *Eur J Nucl Med Mol Imaging.* 2015;42:328–354.
30. Ahmadzadehfar H, Zimbelmann S, Yordanova A, et al. Radioligand therapy of metastatic prostate cancer using ^{177}Lu-PSMA-617 after radiation exposure to ^{223}Ra-dichloride. *Oncotarget.* 2017;8:55567–55574.
31. Heck MM, Retz M, D'Alessandria C, et al. Systemic radioligand therapy with Lu-PSMA-I&T in patients with metastatic castration-resistant prostate cancer. *J Urol.* 2016;196:382–391.
32. Rahbar K, Boegemann M, Yordanova A, et al. PSMA targeted radioligand therapy in metastatic castration resistant prostate cancer after chemotherapy, abiraterone and/or enzalutamide: a retrospective analysis of overall survival. *Eur J Nucl Med Mol Imaging.* 2018;45:12–19.
33. Hofman MS, Violet J, Hicks RJ, et al. [^{177}Lu]-PSMA-617 radionuclide treatment in patients with metastatic castration-resistant prostate cancer (LuPSMA trial): a single-centre, single-arm, phase 2 study. *Lancet Oncol.* 2018;19:825–833.
34. Fendler WP, Eiber M, Beheshti M, et al. Ga-PSMA PET/CT: joint EANM and SNMMI procedure guideline for prostate cancer imaging: version 1. 0. *Eur J Nucl Med Mol Imaging.* 2017;44:1014–1024.
35. Delker A, Fendler WP, Kratochwil C, et al. Dosimetry for ^{177}Lu-DKFZ-PSMA-617: a new radiopharmaceutical for the treatment of metastatic prostate cancer. *Eur J Nucl Med Mol Imaging.* 2016;43:42–51.
36. Christou A, Papastavrou E, Merkouris A, Frangos S, Tamana P, Charalambous A. Clinical studies of nonpharmacological methods to minimize salivary gland damage after radioiodine therapy of differentiated thyroid carcinoma: systematic review. *Evid Based Complement Alternat Med.* 2016;2016:6795076.
37. Wyszomirska A. Iodine-131 for therapy of thyroid diseases: physical and biological basis. *Nucl Med Rev Cent East Eur.* 2012;15:120–123.
38. Kam BL, Teunissen JJ, Krenning EP, et al. Lutetium-labelled peptides for therapy of neuroendocrine tumours. *Eur J Nucl Med Mol Imaging.* 2012;39(suppl 1):S103–S112.
39. Rahbar K, Afshar-Oromieh A, Jadvar H, Ahmadzadehfar H. PSMA theranostics: current status and future directions. *Mol Imaging.* 2018;17:1536012118776068.
40. Emmett L, Willowson K, Violet J, Shin J, Blanksby A, Lee J. Lutetium 177 PSMA radionuclide therapy for men with prostate cancer: a review of the current literature and discussion of practical aspects of therapy. *J Med Radiat Sci.* 2017;64:52–60.
41. Jentzen W, Richter M, Nagarajah J, et al. Chewing-gum stimulation did not reduce the absorbed dose to salivary glands during radioiodine treatment of thyroid cancer as inferred from pre-therapy ^{124}I PET/CT imaging. *EJNMMI Phys.* 2014;1:100.
42. Liu B, Kuang A, Huang R, et al. Influence of vitamin C on salivary absorbed dose of ^{131}I in thyroid cancer patients: a prospective, randomized, single-blind, controlled trial. *J Nucl Med.* 2010;51:618–623.
43. Fallahi B, Beiki D, Abedi SM, et al. Does vitamin E protect salivary glands from I-131 radiation damage in patients with thyroid cancer? *Nucl Med Commun.* 2013;34:777–786.
44. Hong CM, Son SH, Kim CY, et al. Emptying effect of massage on parotid gland radioiodine content. *Nucl Med Commun.* 2014;35:1127–1131.
45. Nakada K, Ishibashi T, Takei T, et al. Does lemon candy decrease salivary gland damage after radioiodine therapy for thyroid cancer? *J Nucl Med.* 2005;46:261–266.
46. Burlage FR, Roesink JM, Kampinga HH, et al. Protection of salivary function by concomitant pilocarpine during radiotherapy: a double-blind, randomized, placebo-controlled study. *Int J Radiat Oncol Biol Phys.* 2008;70:14–22.
47. Bohuslavizki KH, Brenner W, Klutmann S, et al. Radioprotection of salivary glands by amifostine in high-dose radioiodine therapy. *J Nucl Med.* 1998;39: 1237–1242.
48. Bohn KP, Kletting P, Solbach C, Beer AJ, Krohn T. Effect of salivary gland cooling in therapy with PSMA radioligands [in German]. *Nucl Med (Stuttg).* 2017; 56:A2–A91.
49. Abuqbeitah M, Demir M, Uslu-Beşli L, Yeyin N, Sönmezoğlu K. Blood clearance and occupational exposure for ^{177}Lu-DOTATATE compared to ^{177}Lu-PSMA radionuclide therapy. *Radiat Environ Biophys.* 2018;57:55–61.
50. Morris MJ, Pandit-Taskar N, Carrasquillo JA, et al. Phase I trial of zirconium 89 (Zr89) radiolabeled J591 in metastatic castration-resistant prostate cancer (mCRPC) [abstract]. *J Clin Oncol.* 2013;31(suppl):31.
51. Bander NH, Milowsky MI, Nanus DM, Kostakoglu L, Vallabhajosula S, Goldsmith SJ. Phase I trial of ^{177}lutetium-labeled J591, a monoclonal antibody to prostate-specific membrane antigen, in patients with androgen-independent prostate cancer. *J Clin Oncol.* 2005;23:4591–4601.
52. Baum RP, Langbein T, Singh A, et al. Injection of botulinum toxin for preventing salivary gland toxicity after PSMA radioligand therapy: an empirical proof of a promising concept. *Nucl Med Mol Imaging.* 2018;52:80–81.
53. Hakim SG, Benedek GA, Su Y-X, et al. Radioprotective effect of lidocaine on function and ultrastructure of salivary glands receiving fractionated radiation. *Int J Radiat Oncol Biol Phys.* 2012;82:e623–e630.
54. Kratochwil C, Giesel FL, Leotta K, et al. PMPA for nephroprotection in PSMA targeted radionuclide therapy of prostate cancer. *J Nucl Med.* 2015;56: 293–298.